MSC-01566

NATIONAL AERONAUTICS AND SPACE ADMINISTRATION

MSC INTERNAL NOTE NO. 70-FM-22

Feburary 25, 1970

OPTIMUM TWO-DIMENSIONAL SINGLE-STAGE LAUNCH FROM THE SURFACE OF MARS

Advanced Mission Design Branch

MISSION PLANNING AND ANALYSIS DIVISION

MANNED SPACECRAFT CENTER

HOUSTON, TEXAS

MSC INTERNAL NOTE NO. 70-FM-22

OPTIMUM TWO-DIMENSIONAL SINGLE-STAGE LAUNCH FROM THE SURFACE OF MARS

By Thomas B. Murtagh
Advanced Mission Design Branch

February 25, 1970

MISSION PLANNING AND ANALYSIS DIVISION
NATIONAL AERONAUTICS AND SPACE ADMINISTRATION
MANNED SPACECRAFT CENTER
HOUSTON, TEXAS

Approved: Jack Funk
Jack Funk, Chief
Advanced Mission Design Branch

Approved: John P. Mayer
John P. Mayer, Chief
Mission Planning and Analysis Division

CONTENTS

FIGURES

OPTIMUM TWO-DIMENSIONAL SINGLE-STAGE LAUNCH FROM THE SURFACE OF MARS

By Thomas B. Murtagh

1.0 SUMMARY

A detailed mathematical description of the optimization procedures used to generate two-dimensional single-stage launch trajectories is presented. A typical velocity budget for a launch from the surface of Mars is developed to illustrate the theory. This trajectory consists of a 10-second vertical rise followed by a time-optimum transfer to an intermediate orbit which has an apoapsis altitude of 100 n. mi. For the cases considered, the launch velocity requirement was between 14 000 and 15 500 fps.

2.0 INTRODUCTION

The mission plan and systems model which might be used to fly a manned mission to Mars is discussed in considerable detail in reference 1. Some of the mission objectives outlined in that reference involve unmanned and manned landing vehicles to research and explore the Martian surface. The retrieval of these vehicles by a launch from the surface to some intermediate parking orbit is the subject of this note. The lander is assumed to coast in the intermediate orbit and then to execute a series of maneuvers to rendezvous with the main spacecraft in its Mars parking orbit. A subsequent analysis will be performed to calculate these rendezvous maneuvers.

The analysis presented here is an extension of the preliminary performance estimates provided in reference 2. It that reference, a time-optimum, range-free trajectory program, which assumed constant thrust, was used to obtain the data. However, the atmospheric drag terms were included only in the dynamical equations of motion and were omitted in the equations which provide the feedback control for shaping the optimum trajectory. This mathematical limitation was removed for the current analysis. The purpose of this analysis is (1) to provide a detailed mathematical description of the optimization procedures and

convergence techniques used to generate the numerical data, and (2) to discuss some typical performance data which provide the motivation for the ultimate choice of the characteristics of the intermediate parking orbit for the lander. These parking orbit characteristics will be used in a subsequent analysis to develop a launch window profile for the lander.

3.0 SYMBOLS

A	vehicle cross-sectional area
C_D	drag coefficient
C	matrix defined in eq. (54)
E	energy of orbit
f	vector function defined in eq. (10)
f_1, f_2, f_3, f_4	components of f
F	vector defined by eq. (13)
F_1, F_2	components of F
g	vector function defined by eq. (43)
h	vector function defined by eq. (44)
H	generalized Hamiltonian defined by eq. (9)
I	identity matrix
L	angular momentum of orbit
m	vehicle mass
r	radial position (fig. 1)
T	vehicle thrust
t	time
u	radial velocity (fig. 1)

v	tangential velocity (fig. 1)
W_o	initial vehicle weight
x	state vector defined by eq. (11)
y	correction vector defined by eq. (53)
z	augmented state vector defined by eq. (13)
α	parameter defined by eq. (55)
β	angle between thrust and local horizontal
ϵ	parameter defined by eq. (57)
Γ	transition matrix [eq. (49) and (50)]
θ	angular position (fig. 1)
ρ	atmospheric density
λ	Lagrange multiplier vector
$\lambda_1, \lambda_2, \lambda_3, \lambda_4$	components of λ
μ	gravitational constant times mass of central body
ξ	parameter defined by eq. (52)
η	true anomaly

Subscripts

$B_{(\ )}$	partial derivative of B with respect to ( )
f	final value
o	initial value

Superscripts

T	transpose operator
$\dot{(\ )}$	derivative of ( ) with respect to time
-1	inverse operator

Operators

d( )	differential of ( )
δ( )	variation of ( )
DIAG( )	diagonal of ( )

4.0 ANALYSIS

4.1 State and Co-State Differential Equations

The nonlinear ordinary differential equations of motion for the two-dimensional, minimum-time, constant-thrust launch trajectory are shown by equations (1) through (4) (ref. 3).

$$\dot{u} = \frac{v^2}{r} - \frac{\mu}{r^2} + \left(\frac{T}{m}\right) \sin \beta - \frac{\rho C_D A u \sqrt{u^2 + v^2}}{2m} \tag{1}$$

$$\dot{v} = -\frac{uv}{r} + \left(\frac{T}{m}\right) \cos \beta - \frac{\rho C_D A v \sqrt{u^2 + v^2}}{2m} \tag{2}$$

$$\dot{r} = u \tag{3}$$

$$\dot{\theta} = \frac{v}{r} \tag{4}$$

where u, v, r, and θ are the radial velocity, tangential velocity, radial position, and angular position, respectively (fig. 1). The control variable β is the thrust orientation with respect to the local horizontal; $m = m_0 - \dot{m}t$ is the vehicle mass; and $\rho = \rho(r)$ is the density of the atmosphere. The drag coefficient C_D and the vehicle cross-sectional area A are assumed constant. The Euler-Lagrange (costate) differential equations are represented by equations (5) through (8).

$$\dot{\lambda}_1 = \lambda_1 \left[\frac{\rho C_D A(2u^2 + v^2)}{2m\sqrt{u^2 + v^2}} \right] + \lambda_2 \left[\frac{\rho C_D A u v}{2m\sqrt{u^2 + v^2}} + \frac{v}{r} \right] - \lambda_3 \tag{5}$$

$$\dot{\lambda}_2 = -\lambda_1 \left[\frac{2v}{r} - \frac{\rho C_D A u v}{2m\sqrt{u^2 + v^2}} \right] + \lambda_2 \left[\frac{\rho C_D A(u^2 + 2v^2)}{2m\sqrt{u^2 + v^2}} + \frac{u}{r} \right] - \frac{\lambda_4}{r} \tag{6}$$

$$\dot{\lambda}_3 = -\lambda_1 \left[\frac{2\mu}{r^3} - \left(\frac{v}{r}\right)^2 - \frac{C_D A u \sqrt{u^2 + v^2}}{2m} \frac{\partial \rho}{\partial r} \right] - \lambda_2 \left[\frac{uv}{r^2} - \frac{C_D A v \sqrt{u^2 + v^2}}{2m} \frac{\partial \rho}{\partial r} \right] + \lambda_4 \left(\frac{v}{r^2}\right) \tag{7}$$

$$\dot{\lambda}_4 = 0 \tag{8}$$

The generalized Hamiltonian is given in equation (9)

$$H = \lambda^T f \tag{9}$$

where

$$f = \begin{bmatrix} f_1 \\ f_2 \\ f_3 \\ f_4 \end{bmatrix} = \begin{bmatrix} \dot{u} \\ \dot{v} \\ \dot{r} \\ \dot{\theta} \end{bmatrix} = f(x, \beta, t) \tag{10}$$

$$\text{and } x = \begin{bmatrix} u \\ v \\ r \\ \theta \end{bmatrix} \tag{11}$$

$$\lambda = \begin{bmatrix} \lambda_1 \\ \lambda_2 \\ \lambda_3 \\ \lambda_4 \end{bmatrix}$$

The optimality condition $H_\beta = 0$ produces equation (12).

$$\sin \beta = \frac{\lambda_1}{\pm\sqrt{\lambda_1^2 + \lambda_2^2}}$$

$$\cos \beta = \frac{\lambda_2}{\pm\sqrt{\lambda_1^2 + \lambda_2^2}} \qquad (12)$$

where the term $\sqrt{\lambda_1^2 + \lambda_2^2}$ is the magnitude of the primer vector (ref. 4) in the two-dimensional case. The sign ambiguity on the radicals in equation (12) is resolved by application of the Legendre condition for a minimum, $H_{\beta\beta} > 0$, which requires the selection of the minus sign.

4.2 Perturbation Equations

The use of the method of perturbation functions (MPF) (ref. 3) to generate numerical converged solutions to optimization problems requires the derivation of a set of perturbation equations. An augmented form of the state and costate differential equations is given in equation (13).

$$\dot{z} = \begin{bmatrix} \dot{x} \\ \dot{\lambda} \end{bmatrix} = \begin{bmatrix} H_\lambda{}^T(x,\lambda,t) \\ -H_x{}^T(x,\lambda,t) \end{bmatrix} = \begin{bmatrix} F_1 \\ F_2 \end{bmatrix} = [F] \qquad (13)$$

The perturbation equation is given by equation (14)

$$\dot{\delta z} = \left[\frac{\partial F}{\partial z}\right] \delta z \qquad (14)$$

where

$$\left[\frac{\partial F}{\partial z}\right] = \begin{bmatrix} \frac{\partial F_1}{\partial x} & \frac{\partial F_1}{\partial \lambda} \\ \frac{\partial F_2}{\partial x} & \frac{\partial F_2}{\partial \lambda} \end{bmatrix} \qquad (15)$$

The submatrices required in equation (15) can be computed from

$$\frac{\partial F_1}{\partial x} = f_x - f_\beta H_{\beta\beta}^{-1} H_{\beta x} \tag{16}$$

$$\frac{\partial F_1}{\partial \lambda} = -f_\beta H_{\beta\beta}^{-1} f_\beta^T \tag{17}$$

$$\frac{\partial F_2}{\partial x} = -H_{xx} + H_{x\beta} H_{\beta\beta}^{-1} H_{\beta x} \tag{18}$$

$$\frac{\partial F_2}{\partial \lambda} = -f_x^T + H_{x\beta} H_{\beta\beta}^{-1} f_\beta^T \tag{19}$$

The matrix f_x can be written as shown by equation (20)

$$f_x = \begin{bmatrix} \frac{\partial f_1}{\partial u} & \frac{\partial f_1}{\partial v} & \frac{\partial f_1}{\partial r} & \frac{\partial f_1}{\partial \theta} \\ \frac{\partial f_2}{\partial u} & \frac{\partial f_2}{\partial v} & \frac{\partial f_2}{\partial r} & \frac{\partial f_2}{\partial \theta} \\ \frac{\partial f_3}{\partial u} & \frac{\partial f_3}{\partial v} & \frac{\partial f_3}{\partial r} & \frac{\partial f_3}{\partial \theta} \\ \frac{\partial f_4}{\partial u} & \frac{\partial f_4}{\partial v} & \frac{\partial f_4}{\partial r} & \frac{\partial f_4}{\partial \theta} \end{bmatrix} \tag{20}$$

where f_1, f_2, f_3, f_4 are defined in equation (10). The nonzero partial derivatives required in equation (20) are defined in equation (21) through (29).

$$\frac{\partial f_1}{\partial u} = -\frac{\rho C_D A(2u^2 + v^2)}{2m\sqrt{u^2 + v^2}} \tag{21}$$

$$\frac{\partial f_1}{\partial v} = \frac{2v}{r} - \frac{\rho C_D A u v}{2m\sqrt{u^2 + v^2}} \tag{22}$$

$$\frac{\partial f_1}{\partial r} = -\left(\frac{v}{r}\right)^2 + \frac{2\mu}{r^3} - \frac{C_D A u\sqrt{u^2 + v^2}}{2m}\,\frac{\partial \rho}{\partial r} \tag{23}$$

$$\frac{\partial f_2}{\partial u} = -\frac{v}{r} - \frac{\rho C_D A u v}{2m\sqrt{u^2 + v^2}} \tag{24}$$

$$\frac{\partial f_2}{\partial v} = -\frac{u}{r} - \frac{\rho C_D A(u^2 + 2v^2)}{2m\sqrt{u^2 + v^2}} \tag{25}$$

$$\frac{\partial f_2}{\partial r} = \frac{uv}{r^2} - \frac{C_D A v\sqrt{u^2 + v^2}}{2m}\,\frac{\partial \rho}{\partial r} \tag{26}$$

$$\frac{\partial f_3}{\partial u} = 1 \tag{27}$$

$$\frac{\partial f_4}{\partial v} = \frac{1}{r} \tag{28}$$

$$\frac{\partial f_4}{\partial r} = -\frac{v}{r^2} \tag{29}$$

The partial derivatives given in equations (21) through (29) can be extracted from the appropriate coefficients in equations (5) through (8). The vector f_β is calculated from

$$f_\beta = \begin{bmatrix} \frac{T}{m} \cos \beta \\ -\frac{T}{m} \sin \beta \\ 0 \\ 0 \end{bmatrix} \tag{30}$$

and

$$H_{\beta\beta} = \left(\frac{T}{m}\right)\sqrt{\lambda_1^2 + \lambda_2^2} \tag{31}$$

The vector $H_{\beta x}$ is a null vector, and the symmetric matrix H_{xx} has the form

$$H_{xx} = \begin{bmatrix} H_{uu} & H_{uv} & H_{ur} & H_{u\theta} \\ & H_{vv} & H_{vr} & H_{v\theta} \\ & & H_{rr} & H_{r\theta} \\ & & & H_{\theta\theta} \end{bmatrix} \tag{32}$$

The nonzero second partial derivatives required in equation (32) are computed from equations (33) through (38).

$$H_{uu} = \frac{\rho C_D A}{2m} \quad \frac{\lambda_1(2u^3 + 3uv^2) + \lambda_2 v^3}{(u^2 + v^2)\sqrt{u^2 + v^2}} \tag{33}$$

$$H_{uv} = -\frac{\lambda_2}{r} - \frac{\rho C_D A}{2m} \quad \frac{\lambda_1 v^3 + \lambda_2 u^3}{(u^2 + v^2)\sqrt{u^2 + v^2}} \tag{34}$$

$$H_{ur} = \frac{\lambda_2 v}{r^2} - \frac{\partial \rho}{\partial r} \frac{C_D A}{2m} \left[\frac{\lambda_1(2u^2 + v^2) + \lambda_2 uv}{\sqrt{u^2 + v^2}}\right] \tag{35}$$

$$H_{vv} = \frac{2\lambda_1}{r} - \frac{\rho C_D A}{2m} \left[\frac{\lambda_1 u^3 + \lambda_2(3u^2 v + 2v^3)}{(u^2 + v^2)\sqrt{u^2 + v^2}}\right] \tag{36}$$

$$H_{vr} = -\frac{2\lambda_1 v}{r^2} + \frac{\lambda_2 u}{r^2} - \frac{\lambda_4}{r^2} - \frac{\partial \rho}{\partial r} \frac{C_D A}{2m} \left[\frac{\lambda_1 uv + \lambda_2(u^2 + 2v^2)}{\sqrt{u^2 + v^2}}\right] \tag{37}$$

$$H_{rr} = \lambda_1 \left[\frac{2v^2}{r^3} - \frac{6\mu}{r^4}\right] + \frac{2v}{r^3} \left[\lambda_4 - \lambda_2 u\right] - \frac{\partial^2 \rho}{\partial r^2} \frac{C_D A}{2m} \sqrt{u^2 + v^2} \left[\lambda_1 u + \lambda_2 v\right] \tag{38}$$

4.3 Boundary Conditions

The boundary conditions for the state and costate differential equations (ref. 3) can be expressed as by equations (39a) and (39b).

$$g(z_o, t_o) = 0 \tag{39a}$$

$$h(z_f, t_f) = 0 \tag{39b}$$

where t_o and t_f represent the initial and final times, respectively. It is reasonable to assume that the components of the initial state vector are specified so that

$$x(t_o) - x_o = 0 \tag{40}$$

and the unknown elements of z_o are just the initial values of the Lagrange multipliers λ_o. Equation (40) represents four of the required nine boundary conditions required to solve the two-point boundary value problem characterized by equations (1) through (8). The remaining five boundary conditions are obtained by use of the tranversality condition (ref. 3) at the terminal time t_f. The performance index, which is the function to be extremized, for the launch problem considered in this note is the time of flight $t_f - t_o = t_f$. With this performance index, the transversality condition at t_f becomes

$$-\lambda_f^T \, dx_f + (1 + H)_f \, dt_f = 0 \tag{41}$$

4.3.1 Fixed argument of periapsis and true anomaly.- If the launch is assumed to terminate at a specific point in a particular orbit (fixed state in two dimensions), then the terminal boundary conditions as derived from equation (41) are

$$h(z_f, t_f) = \begin{bmatrix} u(t_f) - u_f \\ v(t_f) - v_f \\ r(t_f) - r_f \\ \theta(t_f) - \theta_f \\ (1 + H)_f \end{bmatrix} = 0 \qquad (42)$$

The initial boundary condition $\lambda_3(t_o) = -1.0$ is used in place of the terminal boundary condition $(1 + H)_f = 0$ so that equations (39) become

$$g(z_o, t_o) = \begin{bmatrix} u(t_o) - u_o \\ v(t_o) - v_o \\ r(t_o) - r_o \\ \theta(t_o) - \theta_o \\ \lambda_3(t_o) + 1 \end{bmatrix} = 0 \qquad (43)$$

and

$$h(x_f, t_f) = \begin{bmatrix} u(t_f) - u_f \\ v(t_f) - v_f \\ r(t_f) - r_f \\ \theta(t_f) - \theta_f \end{bmatrix} = 0 \qquad (44)$$

4.3.2 Free argument of periapsis, fixed true anomaly.- If the launch is assumed to terminate at a specific point in an orbit whose line of apsides is unspecified (i.e., angular position free in the two-dimensional problem considered in this note), the initial boundary conditions are given by equation (43), and the terminal boundary conditions as derived from equation (41) are represented by equation (45).

$$h(z_f, t_f) = \begin{bmatrix} u(t_f) - u_f \\ v(t_f) - v_f \\ r(t_f) - r_f \\ \lambda_4(t_f) \end{bmatrix} = 0 \qquad (45)$$

4.3.3 Free argument of periapsis and true anomaly.- If the launch is assumed to terminate in an orbit whose shape is specified (i.e., semi-major axis and eccentricity) but the position in the orbit and apsidal orientation are unspecified, the initial boundary conditions are again given by equation (43), and the terminal boundary conditions are represented by equation (46).

$$h(z_t, t_f) = \begin{bmatrix} rv - L \\ \frac{u^2 + v^2}{2} - \frac{\mu}{r} - E \\ \frac{\lambda_1}{u}\left(\frac{\mu}{rv} - v\right) + \lambda_2 - \lambda_3\left(\frac{r}{v}\right) \\ \lambda_4 \end{bmatrix} = 0 \qquad (46)$$

where E and L are the energy and angular momentum of the desired orbit.

4.4 Integration Procedures

The numerical integration of equations (1) through (8) requires initial values of the Lagrange multipliers $\lambda(t_o)$ and the state vector $x(t_o)$. The initial state vector $x(t_o)$ is usually specified; reasonable values for $\lambda(t_o)$ must be guessed. From equation (8), it is evident that $\lambda_4(t)$ is a constant. Furthermore, when the argument of periapsis is unspecified [eqs. (45) and (46)] $\lambda_4(t) = 0$. If the argument of periapsis is specified [eq. (44)], an initial guess of $\lambda_4(t_o) = 0$ is usually quite good. Use of equation (43) for the initial boundary conditions constitutes specification of $\lambda_3(t_o)$. Consequently, the only unknown initial multipliers are $\lambda_1(t_o)$ and $\lambda_2(t_o)$. It can be shown (ref. 5) that, for the case in which the argument of periapsis is free, a reasonable calculation of these initial multipliers is provided by equations (47) and (48).

$$\lambda_2(t_o) = \frac{t_f \lambda_3(t_o)}{\tan \beta\,(t_o) - \tan \beta\,(t_f)} \tag{47}$$

$$\lambda_1(t_o) = \lambda_2(t_o) \tan \beta\,(t_o) \tag{48}$$

Some estimate is still required for the initial and final pitch angles $\beta(t_o)$ and $\beta(t_f)$ and the time of flight t_f but these parameters possess more physical significance than do the corresponding Lagrange multipliers. The integration of the state and costate equations of motion with some $z(t_o)$ generally will produce an $h(z_f, t_f)$ which is nonzero. The error is this terminal constraint vector must then be mathematically related to the initial conditions to begin an iteration procedure which will converge on the desired solution.

4.5 Iteration Procedures

If the value of the terminal constraint vector is expanded in a Taylor series about the value obtained on the i^{th} iteration and only first order terms are retained (ref. 6), then equation (49) results.

$$dh\ (z_f,\ t_f) = \left[\frac{\partial h}{\partial z}\right]_f \Gamma(t_f,\ t_o)\ \delta z\ (t_o) + \dot{h}_f\ dt_f \qquad (49)$$

where the transition matrix $\Gamma(t_f,\ t_o)$ is obtained by simultaneous integration of the equation

$$\dot{\Gamma}(t_f,\ t_o) = \left[\frac{\partial F}{\partial z}\right] \Gamma(t_o,\ t_o) \qquad (50)$$

with the equations of motion and the Euler-Lagrange equations subject to the initial conditions $\Gamma(t_o,\ t_o) = I$, where I is the identity matrix. Because the initial state vector $x(t_o)$ and the initial multiplier $\lambda_3(t_o)$ are assumed to be specifed, $\delta x(t_o) = 0$ and equation (49) can be modified to equation (51).

$$dh\ (z_f,\ t_f) = \left[\frac{\partial h}{\partial z}\right]_f \bar{\Gamma}(t_f,\ t_o)\ \delta\bar{\lambda}\ (t_o) + \dot{h}_f\ dt_f \qquad (51)$$

where $\bar{\Gamma}(t_f,\ t_o)$ is a reduced form of $\Gamma(t_f,\ t_o)$ and $\delta\bar{\lambda}\ (t_o)$ is a reduced form of $\delta\lambda\ (t_o)$. The correction to the initial multipliers and the time of flight can be computed directly from equation (51) after $dh\ (z_f,\ t_f)$ is calculated. One approach is to use the fractional correction procedure (FCP) (refs. 3 and 6) which requires that equation (52) be satisfied.

$$dh\ (z_f,\ t_f) = -\xi h(z_f,\ t_f) \qquad (52)$$

where ξ is a number between 0 and 1. The use of small values of ξ in this equation enchances the possiblity of convergence but increases the computer time. Large values of ξ reduce computer time if the solutions on successive iterations are close to the desired solution but the probability of divergence is increased. The minimum-norm correction procedures (MNCP) derived and discussed in reference 6 enhance the convergence probability by producing an iteration procedure which automatically switches from a gradient solution to the classical Newton-Raphson solution as the desired terminal boundary is approached. The equation for the MNCP stepped -α technique (ref. 6) is given in equation (53).

$$y = -\left[C^T C + \alpha \, \mathrm{diag}(C^T C)\right]^{-1} C^T h \tag{53}$$

where $y^T = [\delta\bar{\lambda}(t_o) \vdots dt_f]$ and the matrix C is

$$C = \left[\left(\frac{\partial h}{\partial z}\right)_f \bar{\Gamma}(t_f, t_o) \vdots \dot{h}_f\right] \tag{54}$$

An initial value for α_o is chosen, and equation (55) is used for α in equation (53).

$$\alpha = \alpha_o \left[\frac{|h|^i}{|h|^{max}}\right]^p \tag{55}$$

The equation for the MNCP stepped-ε technique (ref. 6) is given in equation (56)

$$y = -(C^T C + \varepsilon I)^{-1} C^T h \tag{56}$$

where an initial value for ε_o is chosen and ε is computed from equation (57)

$$\varepsilon = \varepsilon_o \left[\frac{|h|^i}{|h|^{max}}\right]^p \tag{57}$$

The parameter $|h|^i$ is the norm of the terminal constraint vector $h(z_f, t_f)$ on the ith iteration, and $|h|^{max}$ is the maximum value of this norm (usually produced on the first iteration). Equations (53) through (57) are derived and discussed in considerable detail in reference 6 and are listed in this note for the sake of completeness.

4.6 Terminal Constraint Vector Derivatives

The partial derivative matrix $\left[\frac{\partial h}{\partial z}\right]_f$ and the total time derivative vector $\dot{h}_f$ required for equation (49) will now be listed for the three terminal orbital configurations considered in this note. The matrix $\left[\frac{\partial h}{\partial z}\right]_f$ has the form shown in equation (58).

$$\left[\frac{\partial h}{\partial z}\right]_f = \begin{bmatrix} \frac{\partial h_1}{\partial u} & \frac{\partial h_1}{\partial v} & \cdots & \frac{\partial h_1}{\partial \lambda_4} \\ \vdots & \vdots & & \vdots \\ \frac{\partial h_4}{\partial u} & \frac{\partial h_4}{\partial v} & \cdots & \frac{\partial h_4}{\partial \lambda_4} \end{bmatrix} \tag{58}$$

and the vector $\dot{h}_f$ is written

$$\dot{h}_f^T = \begin{bmatrix} \dot{h}_1 & \dot{h}_2 & \dot{h}_3 & \dot{h}_4 \end{bmatrix} \tag{59}$$

4.6.1 Fixed argument of periapsis, true anomaly.- The nonzero partial derivatives required in equation (58) are represented by equation (60) and (61).

$$\frac{\partial h_1}{\partial u} = \frac{\partial h_2}{\partial v} = \frac{\partial h_3}{\partial r} = \frac{\partial h_4}{\partial \lambda_4} = 1 \tag{60}$$

$$\dot{h}_f^T = \begin{bmatrix} \dot{u} & \dot{v} & \dot{r} & \dot{\theta} \end{bmatrix} \qquad (61)$$

For this terminal constraint configuration, $\left[\frac{\partial h}{\partial z}\right]_f$ is a 4 by 8 matrix, $\dot{h}_f$ is a four-component vector, and

$$\delta\bar{\lambda}^T(t_o) = \begin{bmatrix} \delta\lambda_1 & \delta\lambda_2 & \delta\lambda_4 \end{bmatrix} \qquad (62)$$

4.6.2 Free argument of periapsis, fixed true anomaly.- For this terminal constraint configuration, the matrix $\left[\frac{\partial h}{\partial z}\right]_f$ has a 3 by 8 dimension (omit the fourth row), and the nonzero partial derivatives are as shown by equation (63)

$$\frac{\partial h_1}{\partial u} = \frac{\partial h_2}{\partial v} = \frac{\partial h_3}{\partial r} = 1 \qquad (63)$$

The three components of $\dot{h}_f$ are

$$\dot{h}_f^T = \begin{bmatrix} \dot{u} & \dot{v} & \dot{r} \end{bmatrix} \qquad (64)$$

and

$$\delta\bar{\lambda}^T(t_o) = \begin{bmatrix} \delta\lambda_1 & \delta\lambda_2 \end{bmatrix} \qquad (65)$$

The multiplier $\lambda_4(t)$ is not used in this option because it is zero for all time.

4.6.3 Free argument of periapsis, true anomaly.- For this terminal constraint configuration, the matrix $\left[\frac{\partial h}{\partial z}\right]_f$ again has a 3 by 8 dimension (omit the fourth row), and the nonzero partial derivatives are represented by equations (66) through (72).

$$\frac{\partial h_1}{\partial v} = r \tag{66a}$$

$$\frac{\partial h_1}{\partial r} = v \tag{66b}$$

$$\frac{\partial h_2}{\partial u} = u \tag{67a}$$

$$\frac{\partial h_2}{\partial v} = v \tag{67b}$$

$$\frac{\partial h_2}{\partial r} = \frac{\mu}{r^2} \tag{67c}$$

$$\frac{\partial h_3}{\partial u} = -\frac{\lambda_1}{u^2}\left(\frac{\mu}{rv} - v\right) \tag{68}$$

$$\frac{\partial h_3}{\partial v} = -\frac{\lambda_1}{u}\left(\frac{\mu}{rv^2} + 1\right) + \lambda_3\left(\frac{r}{v^2}\right) \tag{69}$$

$$\frac{\partial h_3}{\partial r} = -\frac{\lambda_1 \mu}{ur^2 v} - \frac{\lambda_3}{v} \tag{70}$$

$$\frac{\partial h_3}{\partial \lambda_1} = \frac{1}{u}\left(\frac{\mu}{rv} - v\right) \tag{71}$$

$$\frac{\partial h_3}{\partial \lambda_2} = 1 \tag{72a}$$

$$\frac{\partial h_3}{\partial \lambda_3} = -\frac{r}{v} \tag{72b}$$

The components of $\dot{h}_f$ are given by equations (73) through (76).

$$\dot{h}_1 = \dot{r}v + r\dot{v} \tag{73}$$

$$\dot{h}_2 = u\dot{u} + v\dot{v} + \frac{\mu \dot{r}}{r^2} \tag{74}$$

$$\begin{aligned}\dot{h}_3 = {} & \left(\frac{\mu}{rv} - v\right)\cdot\left(\frac{\dot{\lambda}_1}{u} - \frac{\lambda_1 \dot{u}}{u^2}\right) \\ & + \frac{\lambda_1}{u}\left[\frac{\mu}{rv}\left(1 - \frac{\dot{r}}{r} - \frac{\dot{v}}{v}\right) - 2v - \dot{v}\right] \\ & + \dot{\lambda}_2 - \dot{\lambda}_3\left(\frac{r}{v}\right) + \frac{\lambda_3}{v}\left(\frac{\dot{r}v}{v} - \dot{r}\right)\end{aligned} \tag{75}$$

$$\delta\dot{\lambda}^T(t_o) = \left(\delta\lambda_1 \delta\lambda_2\right) \qquad (76)$$

5.0 RESULTS AND DISCUSSION

The Mars atmospheric density profile illustrated in figure 2 was used for all data presented in this analysis. The ascent engine specific impulse I_{sp} was fixed at 380 seconds, and the initial lander ballistic parameter $W_o/C_D A$ was chosen to be 400 lb/ft^2. The apoapsis altitude h_a of the intermediate ellipse was always 100 n. mi. These parameters were arbitrarily chosen to illustrate the optimization techniques. The maximum dynamic pressure calculated for the cases considered was 40 lb/ft^2.

The characteristic velocity V_c for the time-optimum (free argument of periapsis) transfer from the termination of the 10-second vertical rise ($\Delta V \approx 400$ fps) to the specified intermediate orbit is presented in figure 3 as a function of the true anomaly η at intermediate orbit insertion. The curves were generated for initial thrust-to-weight ratios T/W_o between 0.6 and 1.4 (measured in Earth g's). Periapsis altitudes h_p of 300 000 feet, 350 000 feet, and 400 000 feet were considered. Lower periapsis altitudes would have produced undesirable orbit decay times for the lander intermediate orbit. Note from these curves that the performance (measured by V_c) is insensitive to variations in true anomaly between -10° and +10°. Consequently, the choice of the true anomaly angle at the intermediate orbit insertion point can be arbitrary within the above limits. With $\eta = +5°$, the characteristic velocity was plotted against the initial thrust-to-weight ratio in figure 4. The minimum V_c's obviously occur for the lowest periapsis altitude (because the apoapsis altitude is fixed at 100 n. mi.), and the minimum of that curve is for $0.8 \leq T/W_o \leq 1.0$. Based on this data, the periapsis altitude of the intermediate ellipse was chosen to be 300 000 feet (for $\eta = +5°$), and the initial thrust-to-weight ratio was chosen to be 1.0 (measured in Earth g's). The ascent and dynamic pressure profile for this case is presented in figure 5.

6.0 CONCLUSIONS

A detailed mathematical description of the optimization procedures used to generate two-dimensional single-stage launch trajectories has been presented. A typical velocity budget for a launch from the surface of Mars was developed. The trajectory consisted of a 10-second vertical rise which required approximately 400 fps followed by a time-optimum transfer to an intermediate orbit which had an apoapsis altitude of 100 n. mi. For the cases considered, the total launch velocity requirement was between 14 000 and 15 500 fps. A subsequent analysis will be performed to develop a launch window profile for the lander and will include a calculation of the maneuvers required to rendezvous the lander from its intermediate orbit to the main spacecraft in its Mars parking orbit.

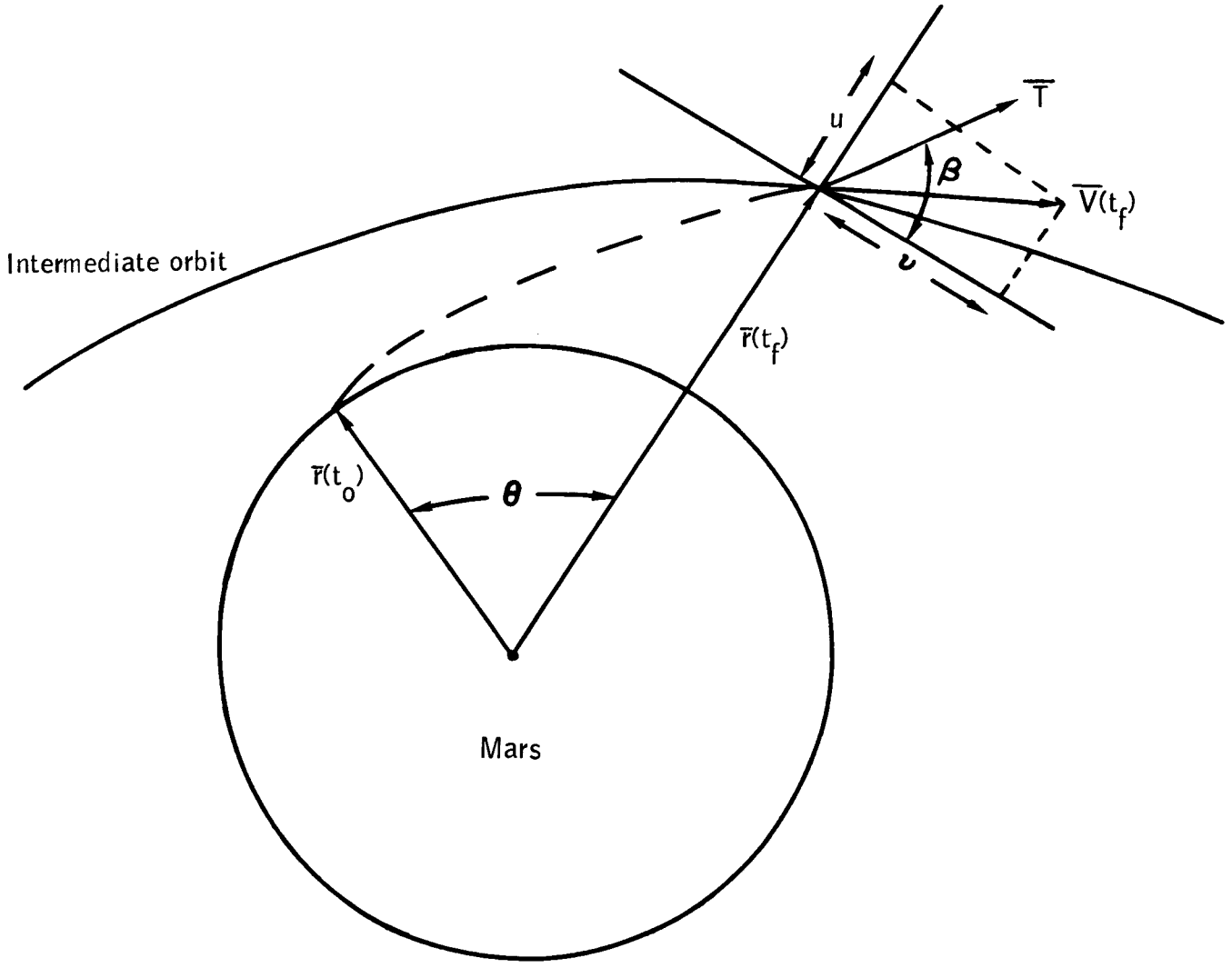

Figure 1.- Geometry of launch trajectory parameters.

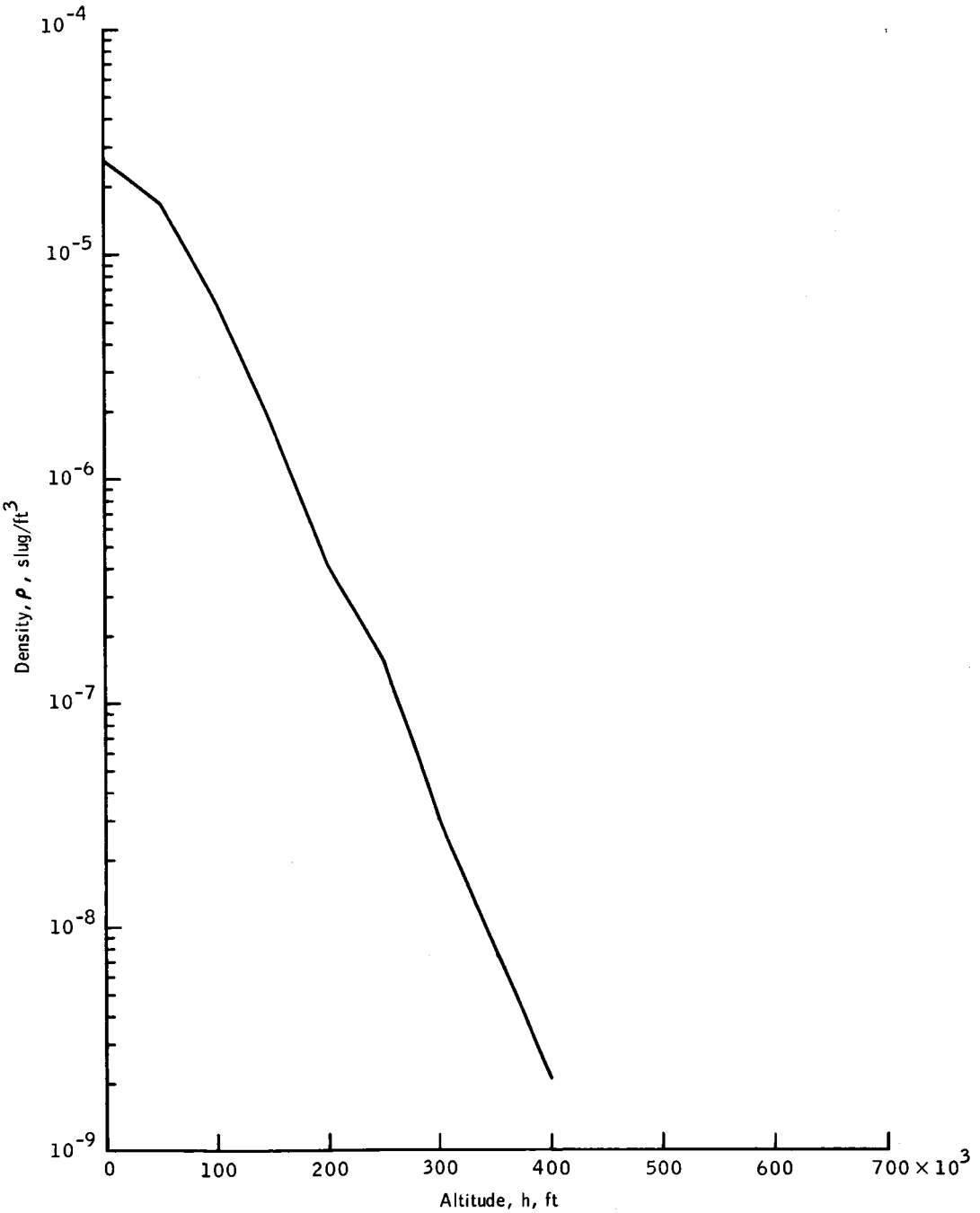

Figure 2.- Mars atmospheric density profile.

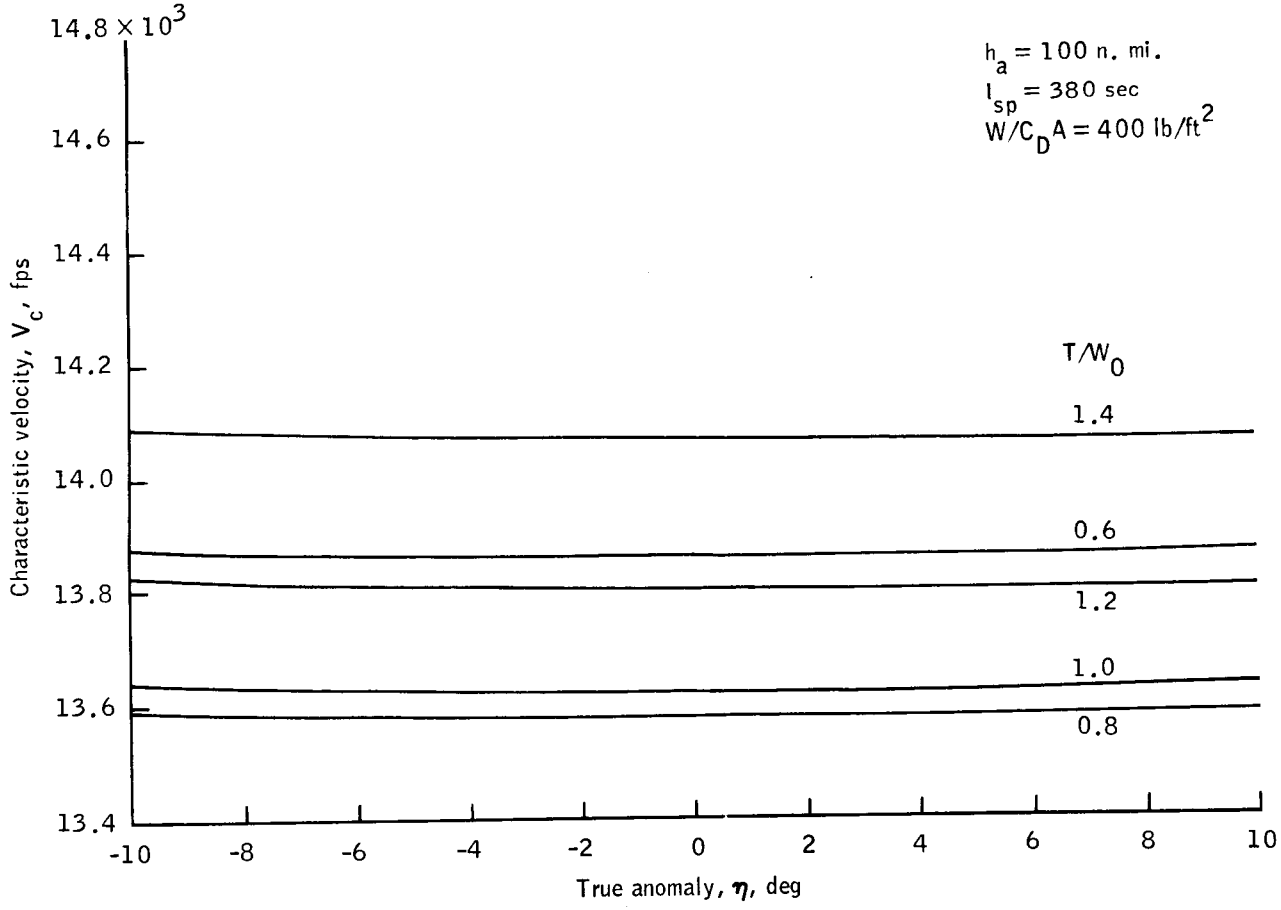

(a) h_p = 300 000 ft.

Figure 3.- Characteristic velocity as a function of true anomaly.

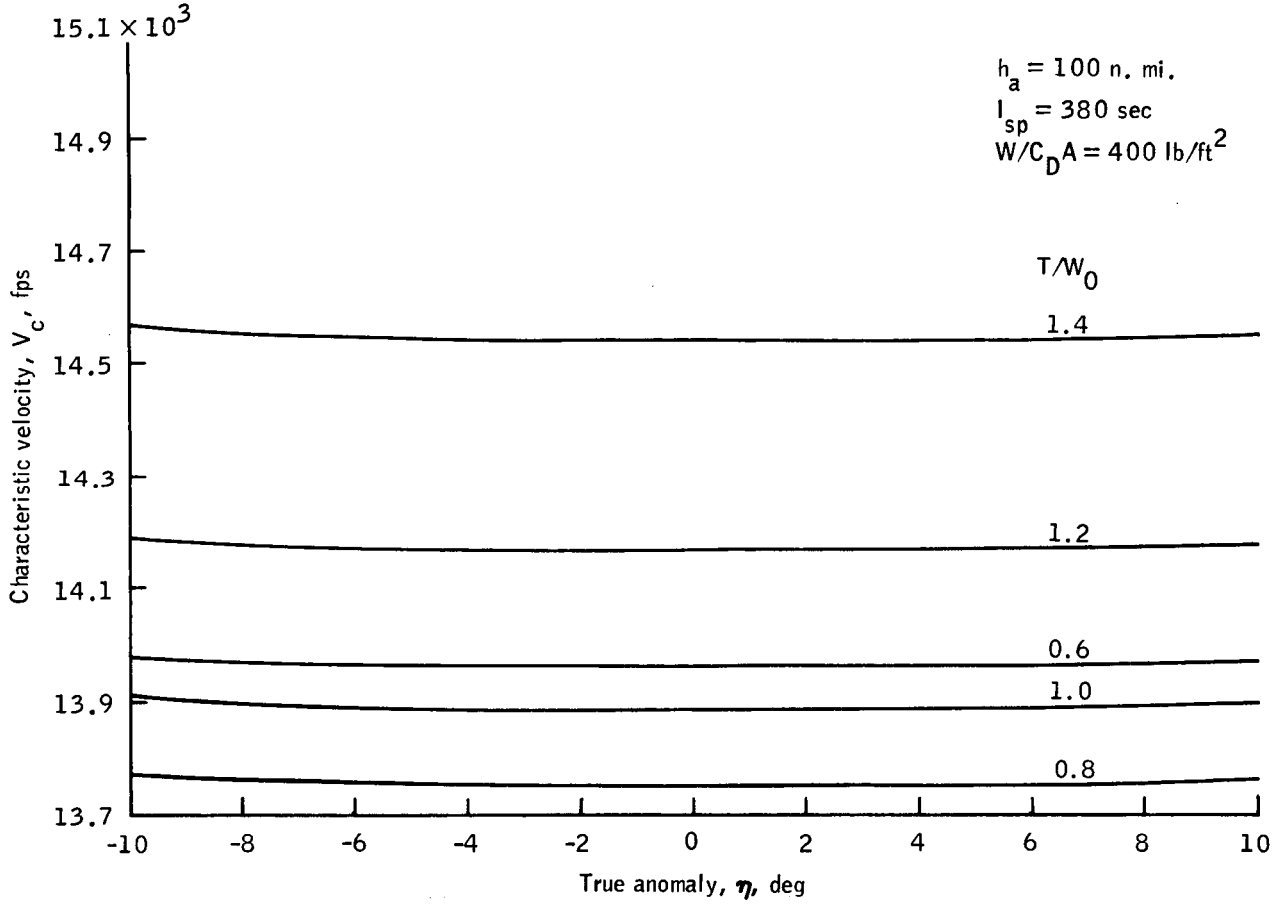

(b) h_p = 350 000 ft.

Figure 3.- Continued.

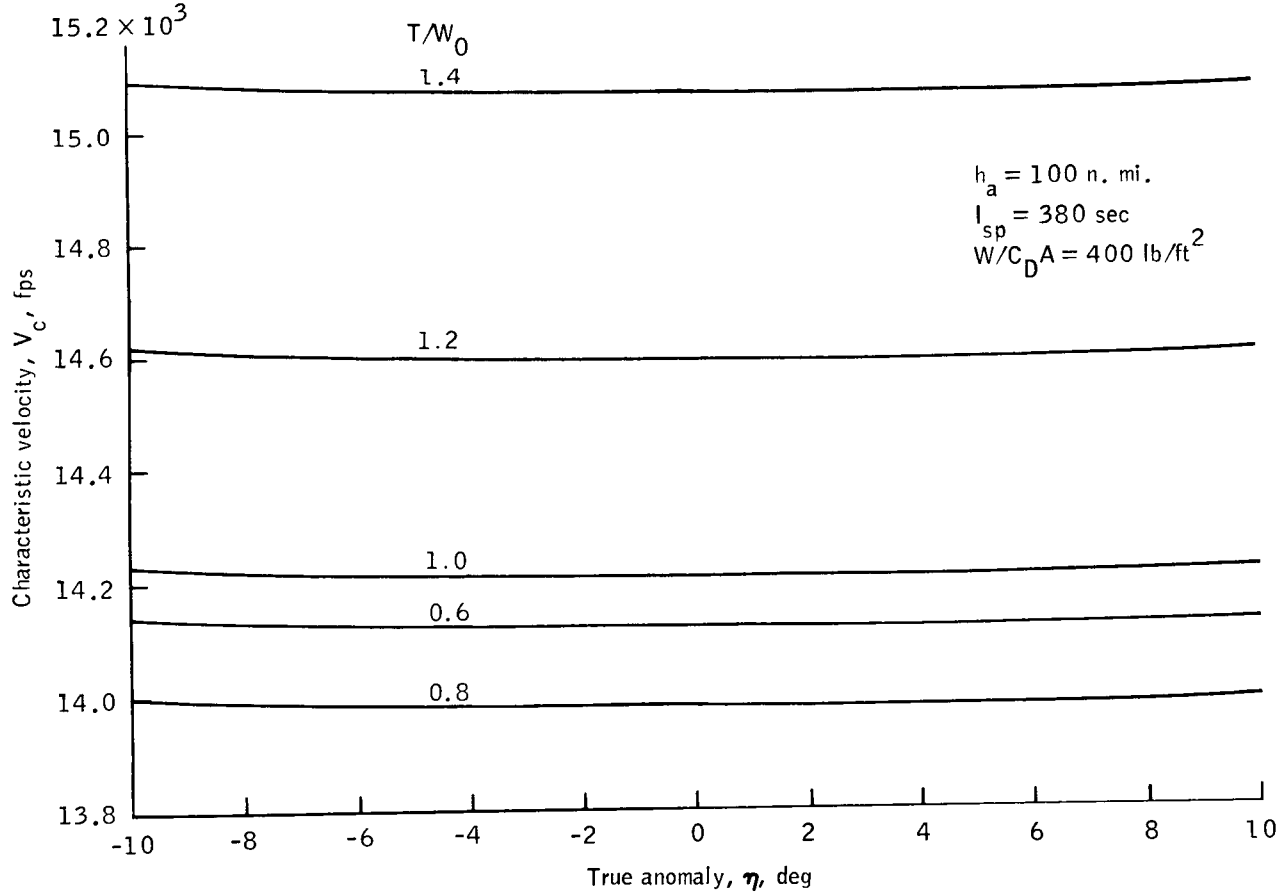

(c) $h_p = 400\ 000$ ft.

Figure 3.- Concluded.

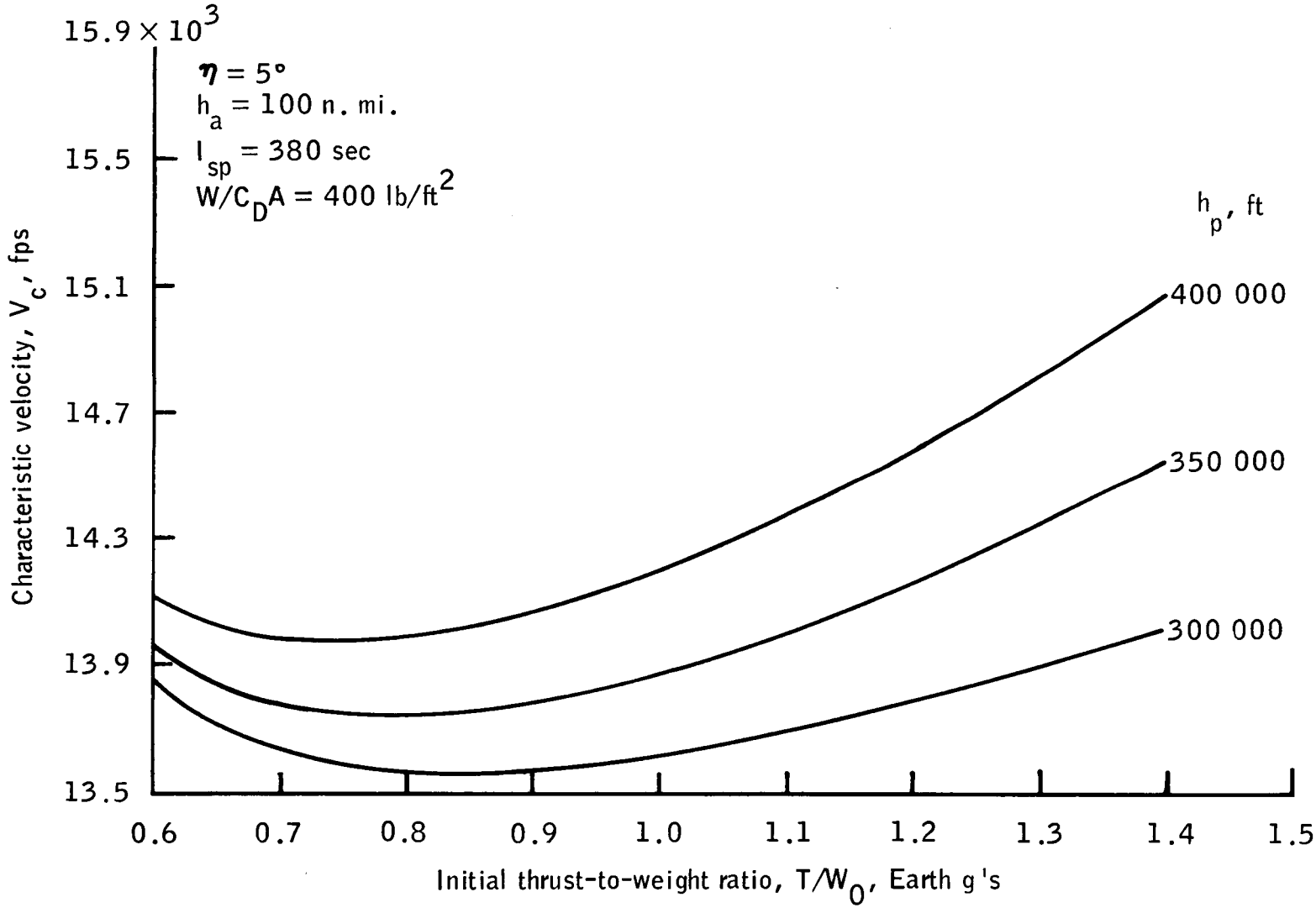

Figure 4.- Characteristic velocity as a function of initial thrust-to-weight ratio.

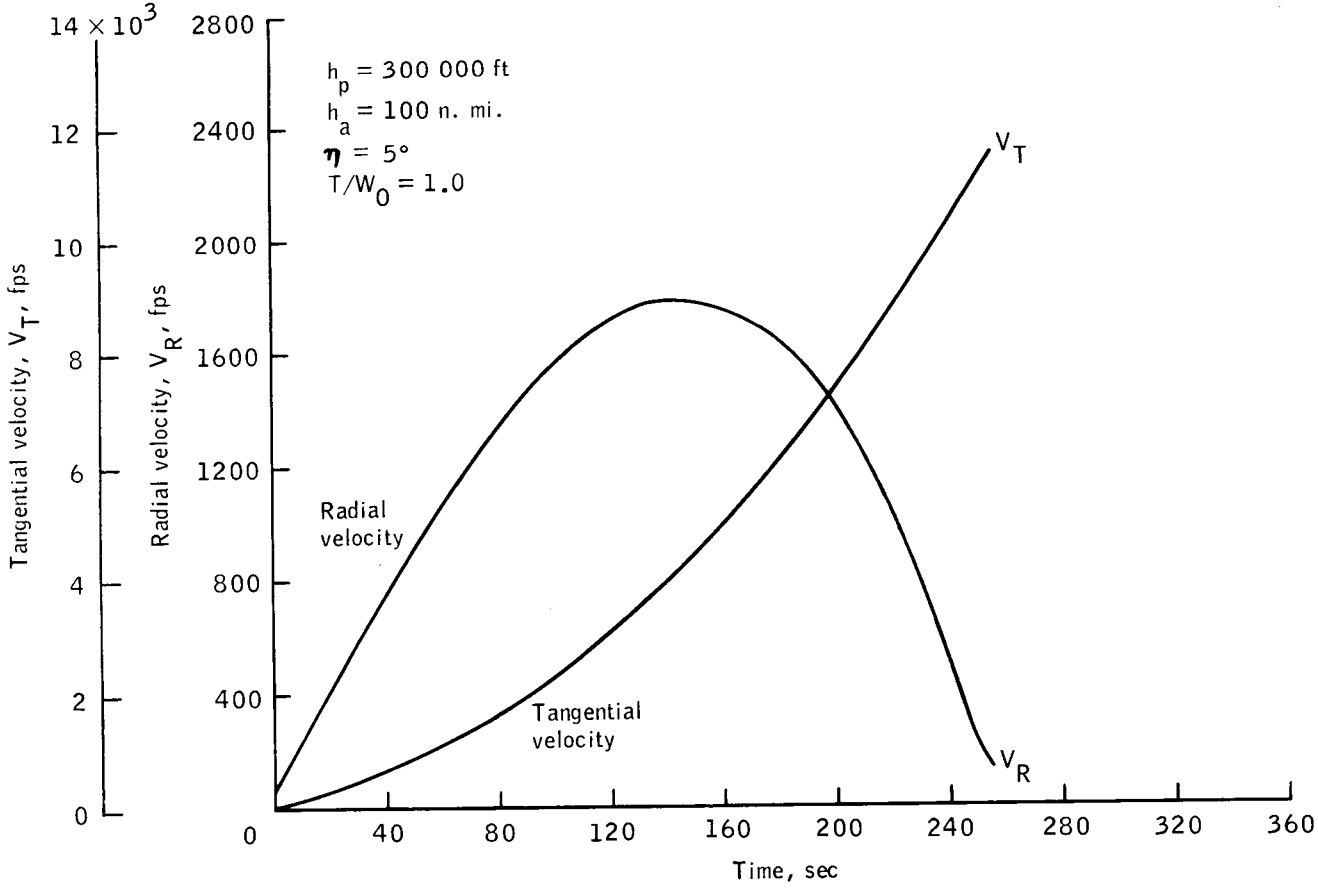

(a) Radial and tangential velocity.

Figure 5.- Typical ascent profile.

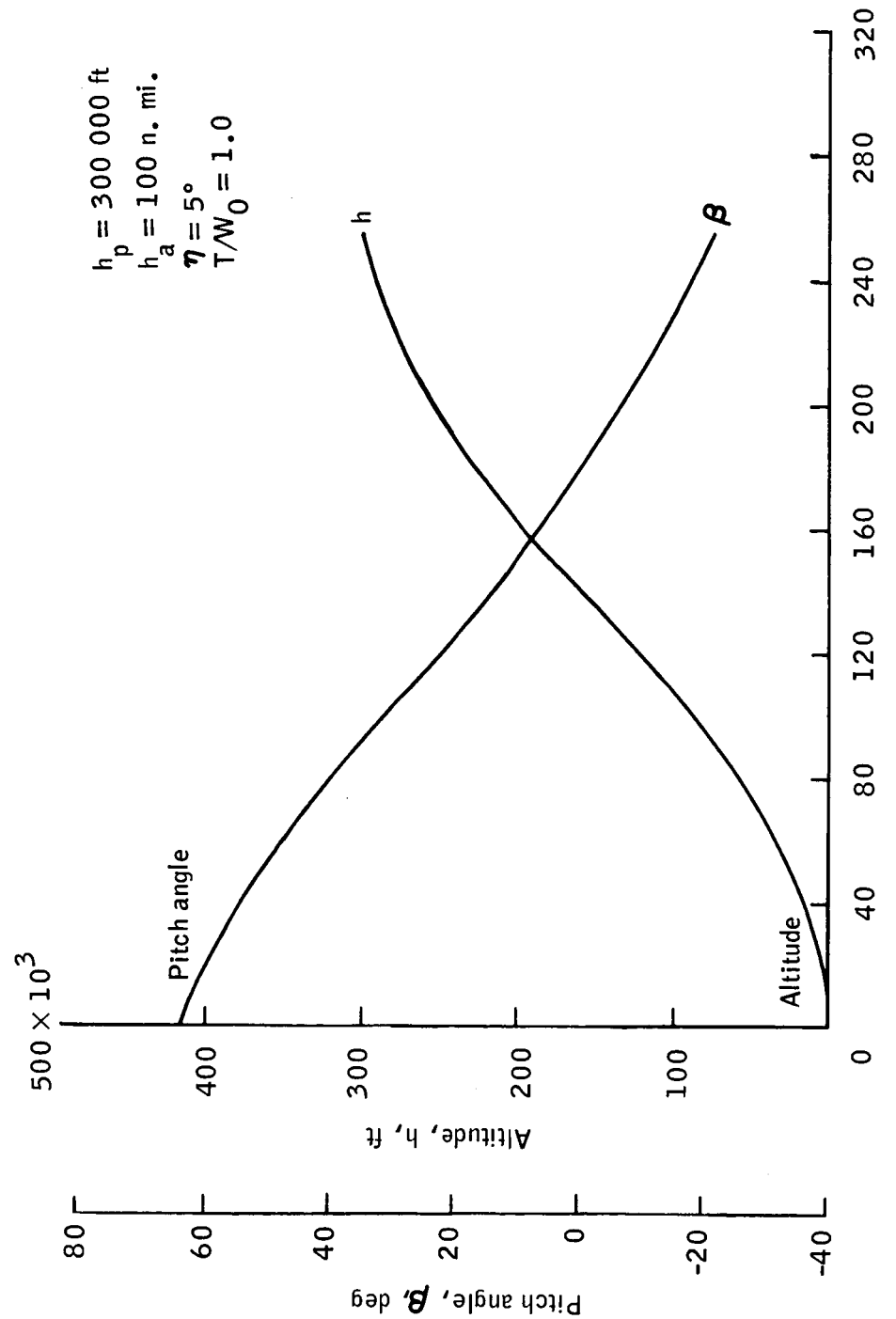

(b) Altitude and pitch angle.

Figure 5.- Continued.

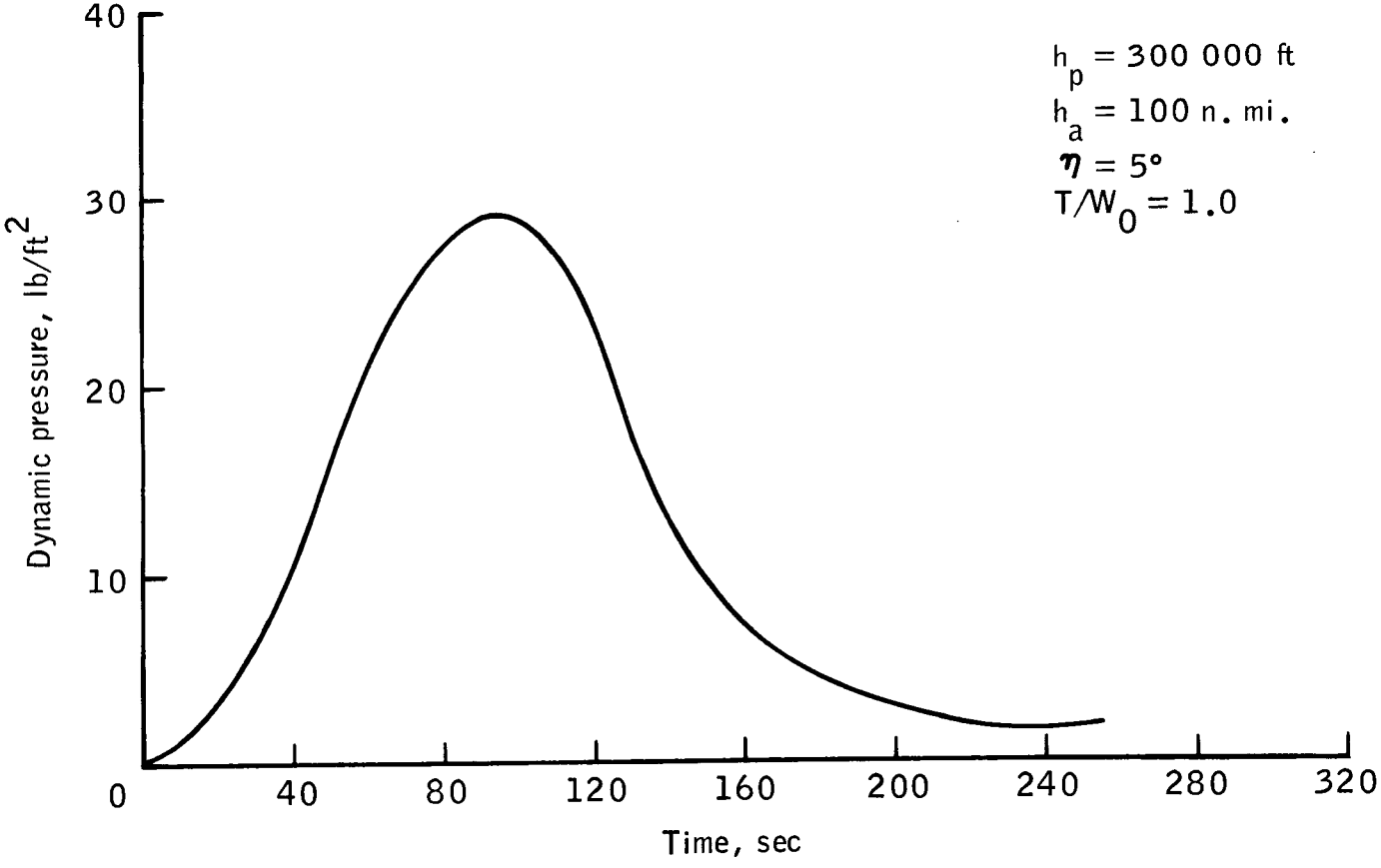

(c) Dynamic pressure.

Figure 5.- Concluded.

REFERENCES

1. Funk, J.; Et Al.: Manned Exploration of Mars: A Minimum-Energy Mission Plan for Maximum Scientific Return. MSC IN 68-FM-70, April 1968.

2. Jezewski, D. J.: Preliminary ΔV Budget for a Launch From the Surface of Mars. MSC IN 66-FM-127, Dec. 1966.

3. Lewallen, J. M.: An Analysis and Comparison of Several Trajectory Optimization Methods. MSC IN 66-ED-43, June 1966.

4. Lawden, D. F.: Optimal Trajectories for Space Navigation. Butterworths (London), 1963.

5. Jezewski, D. J.: Guidance Equations for Quasi-Optimum Space Maneuvers. NASA TN D-2361, Aug. 1964.

6. Lewallen, J. M.; Tapley, B. D.; and Williams, S. D.: Iteration Procedures for Indirect Trajectory Optimization Methods. AIAA Journal of Spacecraft and Rockets, Vol. 5, No. 3, March 1968, pp. 321-327.